

Second-peak effect in a superconducting (Tl, Bi)-1212 single crystal by ac susceptibility: Evidence for vortex plastic behavior

T. Aouaroun and Ch. Simon

Laboratoire CRISMAT, UMR 6508 associée au CNRS, ISMRA et Université de Caen 6, Boulevard du Maréchal Juin, 14050 CAEN Cedex, France

(Received 11 February 1998)

A second peak effect is observed for a (Tl, Bi)-1212 single crystal using ac susceptibility measurements. The analysis of the frequency dependence of the second peak position shows that plasticity governs the vortex dynamics on both sides of the second peak line. This suggests that no particular change in the vortex dynamics occurs by crossing this line. We propose that this second peak effect is due to the temperature activated form of the characteristic relaxation times and to the fact that the characteristic activation energy U_c and the critical current density J_c have inverse variations with the magnetic field B (when one increases with B the other decreases). We also propose that the time dependence of the second peak field position should indicate the vortex dynamics behavior: an increasing second peak field position with time is a fingerprint of elastic behavior while a decreasing second peak field position with time is a fingerprint of plastic behavior. The latter case agrees well with our experimental results. [S0163-1829(98)04441-5]

INTRODUCTION

One of the intriguing effects observable in the high- T_c superconductors (HTCS's) is the anomalous increase in the measured current density with increasing applied magnetic field. This phenomenon is called the second peak (SP) effect. It has been observed in anisotropic superconductors as well as in isotropic ones. In the literature, various interpretations have been proposed to explain this phenomenon such as a change in elastic vortex creep dynamics,^{1,2} field induced pinning mechanism,³ three-dimensional (3D-2D) vortex lattice melting,⁴ and recently elastic vortex creep to plastic vortex creep crossover.^{5,6}

To observe the SP effect, the usual technique is to perform dc magnetization loop measurements at a given temperature. A waiting time is imposed from that the dc field is applied to that a magnetization measurement is recorded. The importance of relaxation effects in the appearance of the SP has been shown by Yeshurun *et al.*⁷ In particular, they have shown that the effect disappears with increased waiting time at relatively high temperatures, while it is built in by increased waiting time at relatively low temperatures.

Among the proposed interpretations, the ones which give a dynamical origin to the observed SP effect are given in Refs. 1, 2 and 7. In the elastic vortex creep change interpretation,^{1,2} the SP field separates the single vortex creep regime below from the bundle vortex creep one above. In such a point of view, the SP effect should be absent at very short time scales ($t \rightarrow t_0$), and the observed one is due to the fact that the relaxation is much faster in the single vortex regime than in the vortex bundle regime.

To explore the response at very short time scales, Harnett *et al.*⁸ have used "pulsing field measurements" which allow for an investigation of the critical state (as $t \rightarrow t_0$). Their measurements, which were performed on (K, Ba)BiO₃, confirmed the presence of the SP effect even for very short time scales ($t_0 \approx 10^{-4}$ sec), which is in conflict with the elastic

vortex creep change interpretation.

In this work, we propose that the time or the frequency dependence of the SP field can give information on the vortex dynamics nature nearby the phase diagram SP line. Indeed, assuming that the activation energy form is given by

$$U(J, B) = T \ln \left(\frac{t}{t_0} \right) \propto B^\nu f(J). \quad (1)$$

Since the current density works for the depinning of the vortices, $f(J)$ should be a decreasing function. In the elastic vortex creep frame,⁹ $f(J)$ is a power-law function, i.e., $f(J) \propto J^{-\mu}$, where μ is a positive constant and ν is positive. In plastic vortex creep $f(J)$ is expected to have a finite value at vanishing current density and ν is negative.^{5,10,11} The time dependence of a characteristic field (the SP field, for example) for a given current density, is given by

$$B \propto \left(\frac{T \ln \left(\frac{t}{t_0} \right)}{f[J(t)]} \right)^{1/\nu}. \quad (2)$$

Thus, according to the shape of the $f(J)$ function and the ν value, the characteristic field B_{SP} will increase or decrease with time.

To investigate a wide range of characteristic times, we have used both dc magnetization loop and ac susceptibility measurements. The relatively high frequency values offer the possibility to probe the short time scales. A similar study has been done by Yamagushi *et al.*¹² in Bi-2212 using dc and ac susceptibility measurements. However, no detailed studies on the time and frequency dependence of the SP field position have been reported to date (to the authors knowledge).

In the present work we report on the observation of the SP effect using ac susceptibility measurements. We have chosen a (Tl, Bi)-1212 single crystal, which has a moderate anisotropy,¹⁹ and exhibits the SP effect, extracted from dc magnetization loops, on a large temperature range approach-

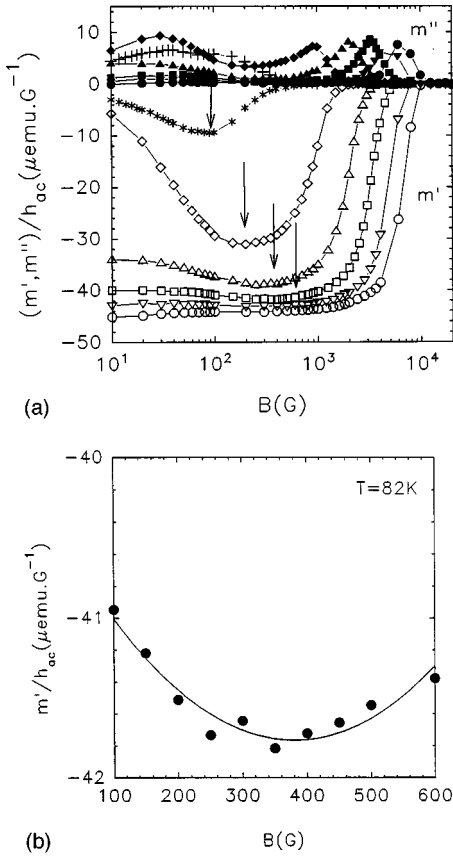


FIG. 1. (a) ac susceptibility versus dc field for temperatures (\circ, \bullet): 78, ($\nabla, \blacktriangledown$): 80, (\square, \blacksquare): 82, ($\triangle, \blacktriangle$): 84, (\diamond, \blacklozenge): 86, and ($*, +$): 88 K. The arrows indicate the ac second peak position. (b) ac SP field extraction using a parabolic fit nearby the minimum of $m'(B)$ at $T=82$ K. The same procedure is used to localize the dc SP field.

ing even the critical temperature. The fact that it is free of twin boundaries permits us to investigate the vortex dynamics in presence of only noncorrelated defects (i.e., without any correlated defects such as twin boundaries or columnar defects). The absence of any observable first order transition in this compound suggests the presence of such defects, which could be, for example, oxygen vacancies.

In the first part of this paper, the ac susceptibility measurements taken in an applied dc field at different temperatures for given frequency are reported. The position, in B - T phase diagram, of the ac SP line is compared to that of the dc one. In the second part, the time and frequency dependences of the SP field are reported and interpreted.

EXPERIMENTAL RESULTS

A (Tl, Bi)-1212 single crystal of $T_c=89$ K and size of $1000 \times 875 \times 200 \mu\text{m}^3$ is studied here. The preparation and structural details can be found elsewhere.¹³ ac susceptibility measurements were performed using the ac option of a superconducting quantum interference device magnetometer, Quantum Design. The ac field strength b_{ac} was fixed to 1 G. Both b_{ac} and B were parallel to each other and to the \vec{c} axis.

In order to extract the ac SP line, the susceptibility was measured versus dc field for different temperatures. The ac frequency was fixed to $f=10^3$ Hz.

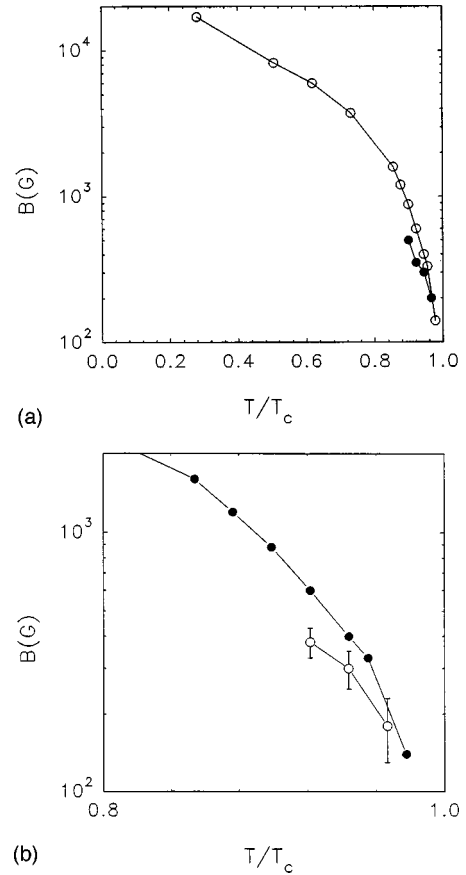


FIG. 2. (a) ac SP line (\bullet) and dc SP one (\circ). One can notice the reduced temperature range of the ac SP line, and its lower position relative to the dc one. (b) Large scale of (a). One can notice that at high temperature the ac SP line joins the dc one.

For each temperature, the measurements begin after that the sample was zero field cooled from above T_c to the studied temperature. After a pause of about 180 sec, the ac susceptibility was recorded versus dc field. A waiting time of 60 sec is imposed after each change of the dc field. Figure 1(a) presents the real and imaginary parts of the ac susceptibility for temperatures going from 78 to 88 K.

For temperatures above 80 K, the real part exhibits a peak effect which is identified to the SP observed in dc magnetization loops. To determine the location of the SP field, a parabolic fit of $m'(B)$ is done nearby the minimum of m' . The ac SP field is then estimated with an error bar of 50 G. Figure 1(b) illustrates this procedure for $T=82$ K. On Fig. 1(a), we can see that the ac SP effect is accompanied by a decrease of the imaginary susceptibility part. This means that the observable current density maximum is reached for a minimum of dissipation. The original behavior of the real part, which presents a maximum, implies the observation of two maxima of the imaginary part since the ‘‘complete penetration’’ of the ac field b_{ac} is reached twice when the dc field varies. The couples (B_{SP}, T_{SP}) corresponding to the effect are reported in Fig. 2(a). We have also reported on the same figure the SP line extracted from dc magnetization.

We will stress the following two facts.

(a) The reduced temperature range for the observation of the SP effect in ac measurements. Indeed, for temperatures lower than 80 K, the effect is absent. This is due to the fact

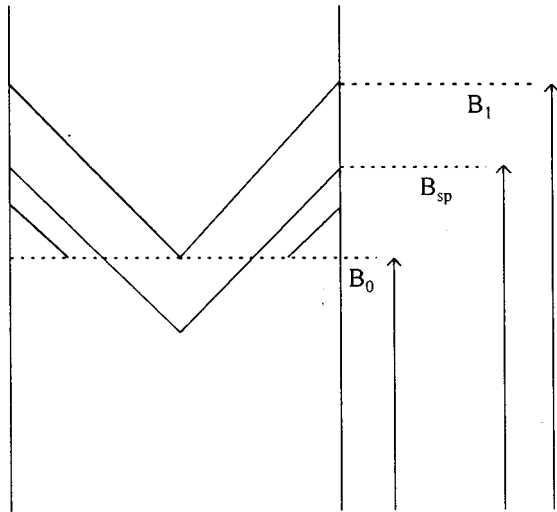


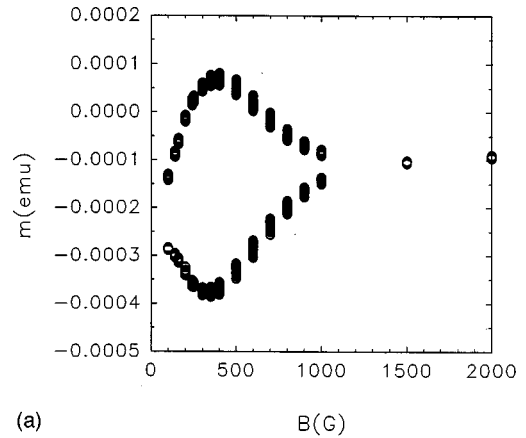
FIG. 3. Illustration of dc global and ac measurements in the case of an infinite slab submitted to a parallel field according to the Bean frame. If B_0 is a characteristic field (the B_{SP} , for example), the effect will be observable for an applied field B_{SP} which is intermediate between B_0 and B_1 in dc measurements. However, the same effect appears for nearly B_0 applied field in surface ac measurements. In fact this approach is approximative since it assumes the simple field independent current density model. The field gradient should be more important near the SP field than near the field of the full penetration.

that at low temperatures, the screening current density is so large that the ac field b_{ac} cannot significantly penetrate the sample. It just probes a negligible part of the sample volume.

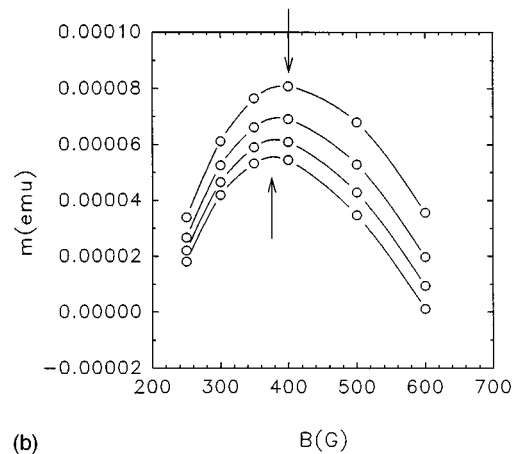
(b) The ac SP line is lower than the dc one. This is due to the global character of dc magnetization measurements. In fact, in the ac susceptibility, if b_{ac} is smaller than the ac complete penetration field but sufficiently large to give a measurable penetrated volume, the probed region will be close to the surface of the sample. Thus the observable peak field (i.e., the applied field where the SP effect occurs B_0) is nearly the local real peak field. In contrast, in global dc magnetization measurements, B_{SP} gives in some way, a mean value between B_0 when the probed region is the surface and B_1 when the probed region is the center of the sample. The scheme reported in Fig. 3 illustrates such a situation in the case of an infinite slab submitted to a parallel field. This approach is very approximative since it assumes the simple field independent current density model. The field gradient should be more important near the SP field than near the field of the full penetration and it is difficult to calculate the exact value of the shift of the ac SP line from the dc one. From Fig. 3, we can see that for small b_{ac} strength, the ac susceptibility gives a good tool to probe the true second peak line. As soon as the temperature is increased, the screening current decreases and the ac superimposed field strength becomes sufficient to probe a larger part of the sample volume, until the entire sample is probed and then the ac SP line rejoins the dc one as it can be seen in Fig. 2(b).

FREQUENCY AND TIME DEPENDENCE OF THE SP LINE

As was pointed out in the introduction, the SP position time or frequency dependence is an indicator of the dissipa-



(a)



(b)

FIG. 4. (a) dc magnetization loop for $T=84$ K. The duration of the relaxation is about 70 min. (b) A zoom of the SP region of the descending branch of (a). The SP field decreases with time as indicated by the arrows. The time criterion is from top to bottom 6, 20, 40, and 70 min.

tion nature near the SP position. To investigate the SP field position time and frequency dependence, we have performed dc magnetization loops with relaxation and ac susceptibility versus field for different frequencies. In the latter case, after a set of measurements for a given frequency, the sample was warmed up to its normal state. After that, it was zero field cooled until the same studied temperature and then a set of measurements for another frequency value began. We report on the Fig. 4(a) a dc magnetization loop for $T=84$ K. The relaxation was performed in 70 min. Figure 4(b) gives a zoom of the descending branch loop near the SP position. As can be seen in this figure, the SP field position decreases with the relaxation. In Fig. 5, the ac real susceptibility part versus field at $T=84$ K is reported for frequencies going from 10^3 to 1 Hz corresponding to characteristic times going roughly from 10^{-3} to 1 sec, i.e., time scales covering three decades. As can be seen, the ac SP field position goes to lower values as the frequency is lowered. The two behaviors, i.e., the decreases of the SP field position with the time and with lowering frequency, indicates probably that plastic behavior is the dominating dynamics near the SP line in (T,Bi)-1212.

In Fig. 6, we report the frequency dependence of the SP field inverse. A satisfactory fit given by

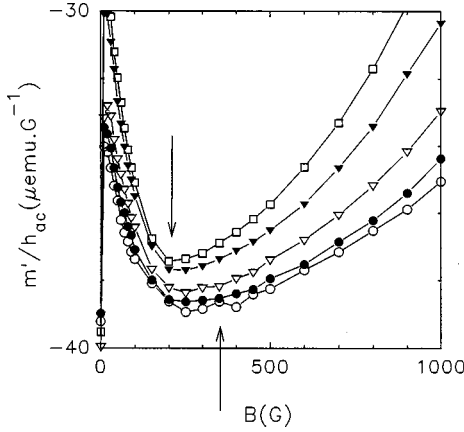


FIG. 5. The real part of ac susceptibility versus field at $T = 84$ K for frequencies 10^3 Hz (\circ), 500 Hz (\bullet), 100 Hz (∇), 10 Hz (\blacktriangledown), and 1 Hz (\square). The SP position is lowered by lowering the frequency as indicated by the arrows.

$$\frac{1}{B_{SP}} = A \ln\left(\frac{f_0}{f}\right) \quad (3)$$

is also represented on the same figure, giving $\nu = -1$. This negative value can be explained assuming plastic creep behavior. The idea according to which the SP line represents a frontier between a B - T diagram domain where the creep is elastic below and another domain where the creep is plastic above^{5,6} should be questioned. The fact that the activation energies are well scaled using two power values ν of opposite signs ($\nu > 0$ for $B < B_{SP}$ and $\nu < 0$ for $B > B_{SP}$) as was done in Refs. 5 and 6, is just due to the relaxation effects.

In fact, it is possible to account for the appearance of the SP effect and its time or frequency dependence, only by assuming opposite field variations of characteristic parameters J_c and U_c . To do so, let us assume that the activation energy for a given temperature is given by

$$U(B, J) = U_c f\left(\frac{J}{J_c}\right), \quad (4)$$

where $f(x)$ is a decreasing function. Assuming the activated form of the characteristic times i.e., $t = t_0 e^{U/T}$, one can write

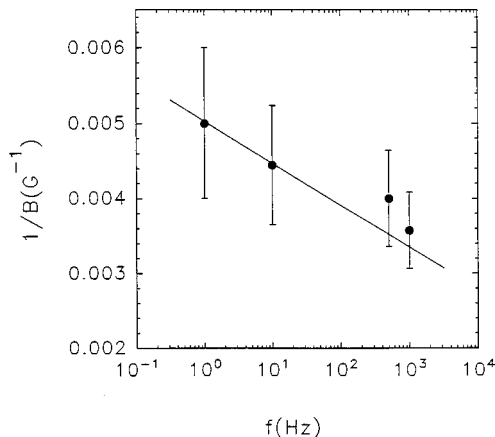
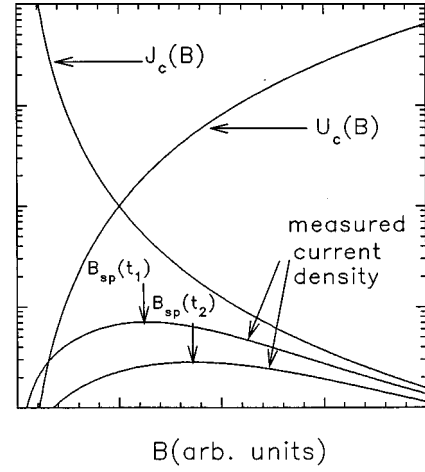
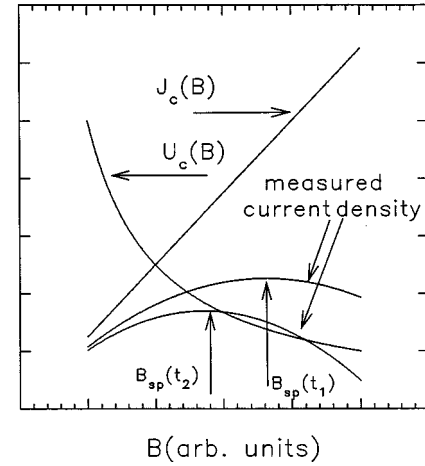


FIG. 6. Frequency dependence of the SP inverse field at $T = 84$ K. The line gives a good fit according to $1/B_{SP} \propto A \ln(f_0/f)$ (see text).



(a)



(b)

FIG. 7. (a) Illustration of relaxation effects for the observation of the SP effect and on its time dependence. The measured current density is described by the interpolation form, i.e.,

$$J = \frac{J_c}{[1 + \mu T \ln(t/t_0)/U_c]} J/\mu$$

with $\mu = 7/9$, $U_c \propto B^3$, and $J_c \propto 1/B^3$ (Ref. 9). One can notice that the SP position increases with time ($t_2 > t_1$). (b) The relaxation effects on SP fields. The measured current density is described by the Anderson model: $J = J_c [1 - T \ln(t/t_0)/U_c]$ with $U_c \propto 1/B$ and $J_c \propto B$ as proposed by Perkins *et al.* (Refs. 14, 16). In this plastic behavior, the SP position decreases with time ($t_2 > t_1$) as it is observed in our experimental measurements.

$$U(B, J) = T \ln\left(\frac{t}{t_0}\right) = U_c f\left(\frac{J}{J_c}\right). \quad (5)$$

For a given experimental time (as in the dc magnetization loop measurements), the measured current density is then given by

$$J = J_c g(B), \quad (6a)$$

where $g(B)$ is given by

$$g(B) = f^{-1}\left(\frac{T \ln(t/t_0)}{U_c(B)}\right). \quad (6b)$$

[We suppose here a weak field dependence of $\ln(t_0)$.]

In the observed time window, a sufficient condition for that a peak in the current density occurs is given by

$$\frac{\partial J}{\partial B} = 0 \Rightarrow \frac{\partial \ln J_c}{\partial B} = - \frac{\partial \ln g}{\partial B}. \quad (7)$$

Thus, it is sufficient that $J_c(B)$ and $g(B)$ have opposite field variations for the SP to occur. Since f is a decreasing function, $f^{-1}(x)$ is also a decreasing one, thus $g(B)$ and $U_c(B)$ have the same field variations. Finally, the previous sufficient condition turns into the following one: $J_c(B)$ and $U_c(B)$ have opposite field variations.

Concerning the time dependence of the SP position, if U_c and J_c present the elastic behavior, i.e., $U_c(B)$ an increasing function and $J_c(B)$ a decreasing one, the observed peak on $J(B)$ increases with the time as illustrated in Fig. 7(a). However, if U_c and J_c have the opposite field dependence of the previous case (we assume this as a plastic behavior), the SP field will decrease with time. This is illustrated in Fig. 7(b). This latter case is similar to that proposed by Perkins *et al.*¹⁴ and it corresponds to our experimental results.

It is possible to describe the behavior of $1/B_{SP}$ vs frequency in a simple way. Let us assume that the activation energy barriers is given simply by the Anderson model,¹⁵ so

$$U(J, B) = U_c \left(1 - \frac{J}{J_c} \right), \quad (8)$$

where we impose that the characteristic activation energy and critical current density vary respectively as $U_c \propto \alpha/B$ and $J_c \propto \beta B$. These field dependences of U_c and J_c correspond to one of the plastic behaviors reported by Perkins *et al.*^{14,16} and used by Jirsa *et al.* to explain their data.¹⁷ On the other hand, supposing an activated form of the characteristic times, one has

$$U(J, B) = T \ln \left(\frac{t}{t_0} \right) = \frac{\alpha}{B} \left(1 - \frac{J}{\beta B} \right). \quad (9)$$

Thus the measured current density is then given by

$$J = J_c \left(1 - \frac{U}{U_c} \right) \propto B \left[1 - \frac{B}{\alpha} T \ln \left(\frac{t}{t_0} \right) \right]. \quad (10)$$

At the maximum of the measured current density, one has $\partial J / \partial B = 0$ and the inverse of SP field is then given by

$$\frac{1}{B_{SP}} = \frac{2T}{\alpha} \ln(t/t_0) = \frac{2T}{\alpha} \ln(f_0/f) = A \ln(f_0/f), \quad (11)$$

where the fit parameters are here $A = 2.43 \times 10^{-4}$ (or 2.43 when B is in T) and $f_0 \approx 9.9 \times 10^8$ Hz. At $T = 84$ K, $B_{SP} = 0.04$ T, so $U_c = \alpha/0.04 = 1730$ K.

This value of U_c can be compared to the energy calculated by Tinkham¹¹ which is involved in the movement of a dislocation located near a vortex row which can be pinned. Such energy is estimated to

$$U_{pl} = \frac{1}{2\mu_0} B_c^2 a_0^2 \xi_c = \frac{1}{4\pi\gamma} \varepsilon_0 a_0 \frac{a_0}{\xi_{ab}},$$

where a_0 is the Abrikosov lattice parameter, $\varepsilon_0 = (1/4\pi\mu_0) (\phi_0/\lambda)^2$ is the line energy, and $\gamma = \sqrt{m_c/m_{ab}}$ the electronic anisotropy. We assume that the temperature dependences of London penetration depth λ and the coherence length ξ are given by the following formulas: $\lambda^{-2}(T) = \lambda^{-2}(0)(1 - T/T_c)$ and $\xi_{ab}^{-2}(T) = \xi_{ab}^{-2}(0)(1 - T/T_c)$, where $\lambda(0) = 1630$ Å, $\xi_{ab}(0) = 20$ Å,¹⁸ $\gamma = 12$,¹⁹ and $T_c = 89$ K, we arrive at $U_c \approx 1700$ K which is of the same order of the calculated value from the fit of the ac SP field inverse.

CONCLUSIONS

We reported on the manifestation of the SP effect in (Tl, Bi)-1212 studied by ac susceptibility measurements. Studying the frequency dependence of the SP field, a plastic behavior is evidenced near the second peak field. Such dynamic occurs well below the observed SP line. This means that there is no particular change at the crossing of the observed SP line. Assuming an activated model with an Anderson energy barrier, we have described the frequency dependence of the SP field position. Even in the absence of any peak in $J_c(B)$, our point of view proposes that in (Tl, Bi)-1212, the peak effect on the measured current density $J(B)$ is a consequence of the temperature activated form of the characteristic relaxation times and of the fact that U_c and J_c have opposite field variations.

ACKNOWLEDGMENTS

We thank A. Maignan and C. Martin for providing the crystal of (Tl, Bi)-1212.

- ¹L. Krusin-Elbaum, L. Civale, V. M. Vinokur, and F. Holtzberg, Phys. Rev. Lett. **69**, 2280 (1992).
- ²M. Nideröst, A. Suter, P. Visani, A. C. Mota, and G. Blatter, Phys. Rev. B **53**, 9286 (1996).
- ³M. Daeumling, J. M. Seuntjens, and D. C. Larbalestier, Nature (London) **346**, 332 (1990).
- ⁴V. Hardy, A. Wahl, A. Ruyter, A. Maignan, C. Martin, L. Coudrier, J. Provost, and Ch. Simon, Physica C **232**, 347 (1994).
- ⁵J. Abulafia, A. Shaulov, Y. Wolfus, R. Prozorov, R. Burlachkov, Y. Yeshurun, D. Mayer, E. Zeldov, H. Wühl, V. G. Geshkenbein, and V. M. Vinokur, Phys. Rev. Lett. **77**, 1596 (1996).

- ⁶T. Aouaroun, V. Hardy, and Ch. Simon, Physica C **294**, 42 (1998).
- ⁷Y. Yeshurun, N. Bontemps, L. Burlachkov, and A. Kapitulnik, Phys. Rev. B **49**, 1548 (1994).
- ⁸W. Harnleit, T. Klein, C. Escribe-Filippini, H. Rakoto, J. M. Broto, A. Sulpice, R. Buder, J. Marcus, and W. Schmidbauer, Physica C **267**, 270 (1996).
- ⁹G. Blatter, M. V. Feigelman, V. B. Geshkenbein, A. I. Larkin, and V. M. Vinokur, Rev. Mod. Phys. **66**, 1125 (1994).
- ¹⁰V. Geshkenbein, A. Larkin, M. Feigelman, and V. Vinokur, Physica C **162-169**, 239 (1989).

- ¹¹M. Tinkham, Phys. Rev. Lett. **61**, 1658 (1988).
- ¹²Yugi Yamaguchi, Nobuyuki Aoki, Fumitoshi Iza, and Yoshikazu Nishihata, Physica C **246**, 216 (1995).
- ¹³M. Ledéser, A. Maignan, J. Chardon, C. Martin, Ph. Labbé, M. Hervieu, and B. Raveau, Physica C **232**, 387 (1994).
- ¹⁴G. K. Perkins, L. F. Cohen, A. A. Zukhov, and A. D. Caplin, Phys. Rev. B **51**, 8513 (1995).
- ¹⁵P. W. Anderson, Phys. Rev. Lett. **9**, 309 (1962).
- ¹⁶G. K. Perkins and A. D. Caplin, Phys. Rev. B **54**, 12 551 (1996).
- ¹⁷M. Jirsa, L. Pust, D. Dlouhy, and M. R. Koblischka, Phys. Rev. B **55**, 3276 (1997).
- ¹⁸The determination of $\lambda(T)$ and $\xi(T)$ are made from the analysis of the reversible part of the dc magnetization versus the field at various temperatures.
- ¹⁹F. Warmont, V. Hardy, J. Provost, D. Grebille, and Ch. Simon, Phys. Rev. B **57**, 7485 (1998).